

# B Cell Ligand Discrimination Through a Spreading and Contraction Response

S. J. Fleire,<sup>1</sup> J. P. Goldman,<sup>2,3</sup> Y. R. Carrasco,<sup>1</sup> M. Weber,<sup>1</sup> D. Bray,<sup>3</sup> F. D. Batista<sup>1\*</sup>

B cells recognize foreign antigens by virtue of cell surface immunoglobulin receptors and are most effectively activated by membrane-bound ligands. Here, we show that in the early stages of this process, B cells exhibit a two-phase response in which they first spread over the antigen-bearing membrane and then contract, thereby collecting bound antigen into a central aggregate. The extent of this response, which is both signaling- and actin-dependent, determines the quantity of antigen accumulated and hence the degree of B cell activation. Brownian dynamic simulations reproduce essential features of the antigen collection process and suggest a possible basis for affinity discrimination. We propose that dynamic spreading is an important step of the immune response.

**B** cells are lymphocytes that make soluble antibodies. They are triggered, or activated, by foreign antigens, typically those presented on the surface of other cells. Activation leads to selective proliferation and differentiation into mature antibody-secreting cells and the selection of high-affinity B cells. Membrane-anchored antigens are known to be very effective in driving B cell activation (1, 2) and may constitute the dominant form of anti-

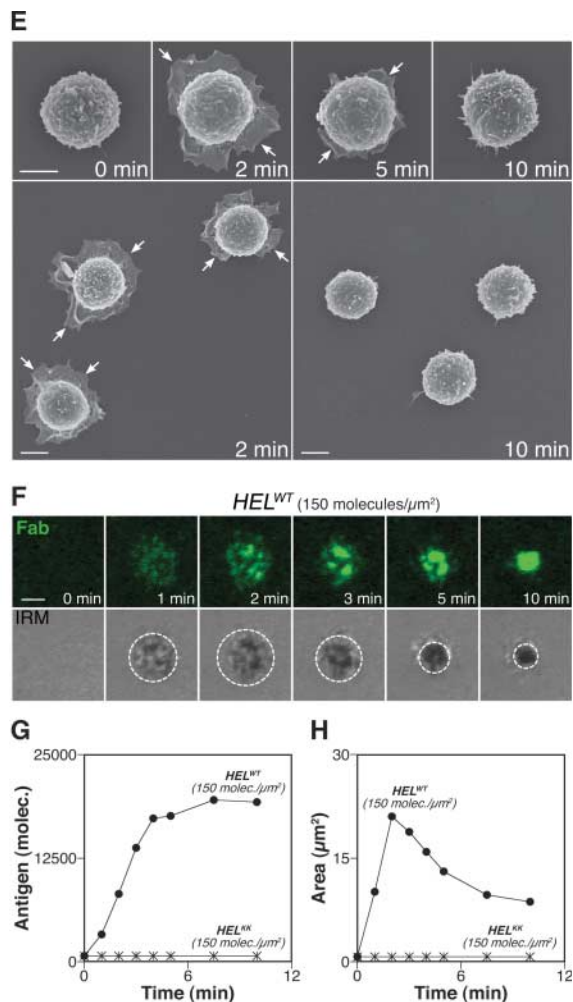
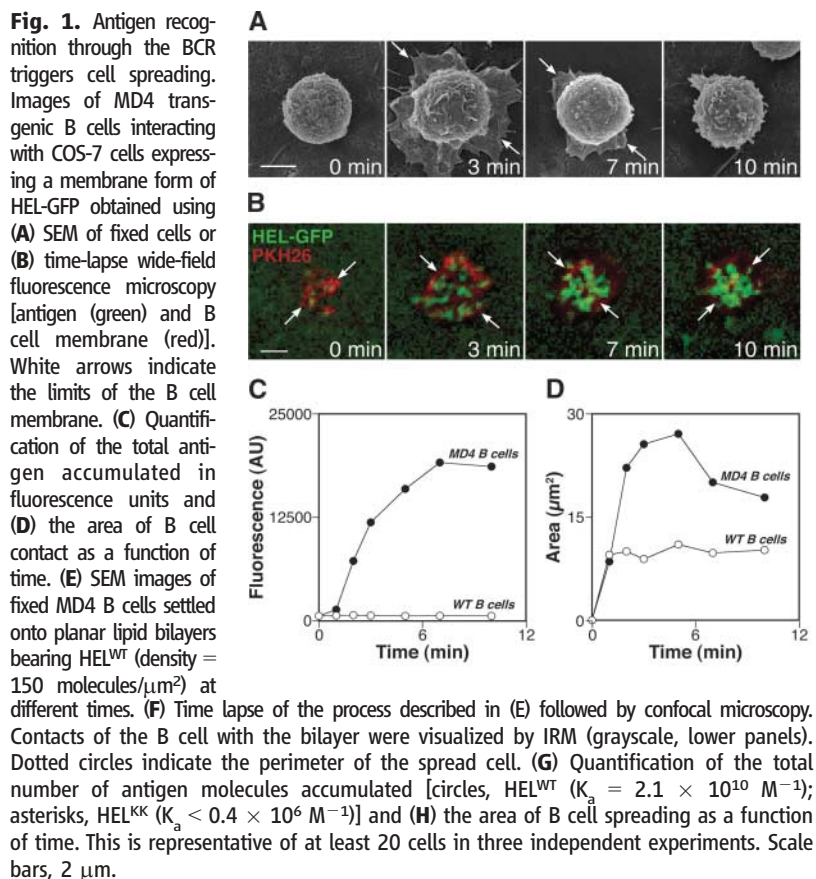
gen responsible for B cell stimulation in vivo (3–7). When a B cell recognizes antigens tethered on the surface of a target cell, a cluster of the B cell receptor (BCR) and its cognate ligand forms at the site of contact (8). Simultaneously, membrane proteins are reorganized on the cell surface, leading to the formation of an immunological synapse. This structure is characterized by a central cluster of BCR/antigen complex surrounded by a ring of adhesion

molecules LFA-1/ICAM-1 (9) and is similar to the synaptic structure originally described for T cells (10–12).

A functional B cell synapse, however, can form in the absence of integrins (8), and this provides an opportunity to quantitatively study the early stages of recognition of membrane-bound antigens. Thus, we observed by scanning electron microscopy (SEM) that when transgenic B cells carrying a BCR specific for hen egg lysozyme (HEL) (13) recognize this antigen on the surface of target cells, they rapidly spread over the target membrane before slowly contracting (Fig. 1A). To follow these morphological changes and relate them to the localization of antigen in real time, we labeled B cell membranes with a lipid soluble dye, PKH26, and expressed the HEL antigen as a fusion protein with green fluorescent protein (GFP) (8). Three-dimensional (3D) time-lapse fluorescence

<sup>1</sup>Lymphocyte Interaction Laboratory, London Research Institute, Cancer Research UK, 44 Lincoln's Inn Fields, London, WC2A 3PX, UK. <sup>2</sup>Computing Laboratory, University of Kent, Canterbury CT2 7NF, UK. <sup>3</sup>Physiology, Development, and Neuroscience, University of Cambridge, Downing Street, Cambridge CB2 3DY, UK.

\*To whom correspondence should be addressed. E-mail: facundo.batista@cancer.org.uk



microscopy revealed that during the spreading phase (2 to 4 min after contact) several small clusters of GFP-HEL of approximately 0.5 to 1  $\mu\text{m}$  in diameter appeared within the area of interaction (Fig. 1B). The flattening B cells reached a maximum surface area of contact of approximately 25  $\mu\text{m}^2$  before gradually starting to contract (Fig. 1, B and C). During this second phase, which lasted for  $\sim 5$  to 7 min, the antigen was gathered into a central defined cluster, with an eventual area of 16  $\mu\text{m}^2$  (Fig. 1D).

Similar morphological changes and kinetics of antigen accumulation were seen when B cells settled on glass-supported planar lipid bilayers (Fig. 1, E to H). In this case, the lysozyme antigen was tethered by a fluorescently labeled glycosylphosphatidylinositol (GPI)-anchored single-chain Fab, which binds to a nonoverlapping epitope of the HEL (fig. S1A). Fluorescence and interference reflection microscopy (IRM), used to examine the dynamics of antigen accumulation and correlate them with changes in cell shape, revealed that this is a general phenomenon that could also be observed with other HEL specific transgenic (14) or transfected B cells (15) (Fig. 1F and fig. S2, A and B).

The cell response was dependent on specific immunological recognition, because the same experiment performed with a null HEL mutant (HEL<sup>KK</sup>) (table S1) with no detectable affinity for the BCR failed to reveal antigen aggregation, contact formation (as assessed by IRM), or any sign of B cell spreading (Fig. 1, G and H). Transgenic B cells carrying a signaling-deficient chimeric BCR (IgM/ $\beta^{\text{Y>L}}$ ) with high affinity binding for the lysozyme (14) or B cells transfected expressing signaling deficient BCRs (15) also showed a complete lack of spreading, and their capacity to accumulate antigen was severely compromised (Fig. 2, A to C, and fig. S2, A to E). Cells carrying the same chimeric receptor but with a functional immunoreceptor tyrosine-based activation motif (ITAM) (16) regained the ability to spread and form antigen aggregates (Fig. 2, A to C). These processes were also blocked when wild-type transgenic B cells were treated with inhibitors of tyrosine kinase or actin polymerization (Fig. 2D). Immunostaining of fixed cells also revealed an accumulation of phosphotyrosine and actin that was coincident with antigen at earliest time points but later moved to the periphery (fig. S2F). Taken together, these results indicate that this is an actin-mediated phenomenon in which both the BCR-antigen binding and functional B cell signaling are required.

The B cell response was sensitive to both the density of antigen in the presenting membrane and the strength of the BCR/antigen interaction. A twofold reduction in the starting density of antigen caused a marked diminution of spreading, and a 10-fold reduction abolished it entirely (Fig. 3A). Using a set of mutant lysozymes with a 20,000-fold range of affinity for BCR (table S1), we found that a  $K_a$  value of

about  $10^6 \text{ M}^{-1}$  is the lower threshold for triggering cell spreading. Above this, the maximum area attained by the B cell increased with its affinity up to a  $K_a$  value of  $5 \times 10^7 \text{ M}^{-1}$  (Fig. 3A). Above the upper threshold, further increases in affinity did not result in additional spreading. Similar results were obtained if we measured the total amount of antigen accumulated (Fig. 3B) or the intracellular calcium levels of the B cells (Fig. 3C). Thus, the magnitude of the signal determines the extent of spreading and ultimately the total amount of antigen accumulated at the end of the response.

The capacity of B cells to extract antigen was assessed using flow cytometry after incubation with HEL-fluorescein isothiocyanate bearing membranes for 2 hours. In these experiments, the amount of antigen acquired was found to be proportional to the total amount of antigen accumulated (Fig. 3D). The ability of B cells to present antigen-derived peptides to T cells was also dependent on the amount of antigen tethered on the membrane (Fig. 3E). Similar

results were obtained when the antigen was presented at different densities on the surface of transfected cells (fig. S3, A to C). Thus, a direct correlation appeared to exist between the amount of antigen accumulated and the capacity of a B cell to extract and present it to T cells.

We next explored the question of how cell spreading enables the cell to detect a wide range of binding affinities using a stochastic computer program in which protein molecules are represented as dimensionless points with Cartesian coordinates and binding radii that determine their interactions during the simulation (17) (Movies S1 to S4). Antigen molecules moved by Brownian diffusion within a square field representing a portion of the lipid bilayer, with periodic boundaries to avoid edge effects. The area of contact between the B cell and the bilayer was represented by a circle, initially small, within which receptors were assigned random positions. These receptors remained fixed in place but, through reversible mass action kinetics, were accessible to diffusing antigens leading to associ-

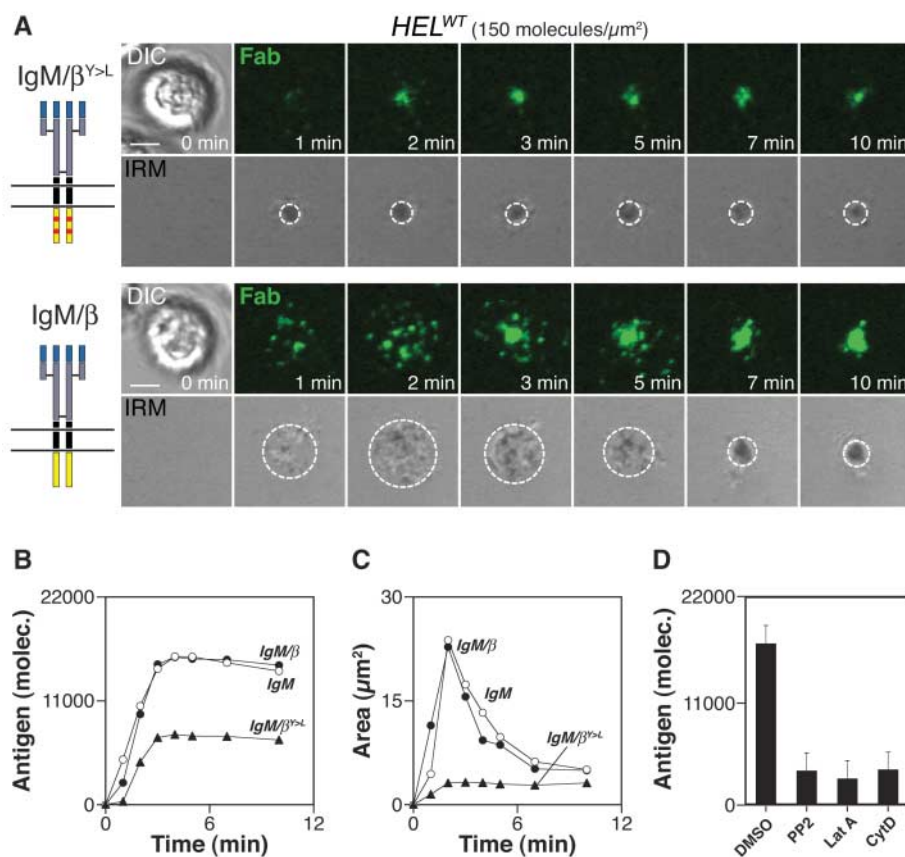


**Fig. 2.** BCR signaling is required for cell spreading and effective antigen collection. (A) Time lapse of the interaction of IgM/ $\beta^{\text{Y>L}}$  (top two panels) and IgM/ $\beta$  (bottom two panels) transgenic naive B cells with artificial lipid bilayers loaded with HEL<sup>WT</sup> antigen (density = 150 molecules/ $\mu\text{m}^2$ ) as followed by confocal microscopy (green) and IRM (gray). Dotted circles indicate the perimeter of the spread cell. Scale bars, 2  $\mu\text{m}$ . (B) Quantification of the total amount of HEL aggregated and (C) the area of B cell spreading for the different transgenic B cells as a function of time. Filled circles, IgM/ $\beta$ ; open circles, IgM; triangles, IgM/ $\beta^{\text{Y>L}}$ . (D) Total amount of accumulated HEL at 10 min when MD4 B cells were treated with the indicated inhibitors. DMSO, dimethylsulfoxide (control); PP2, tyrosine kinase inhibitor; LatA, latrunculin A (actin inhibitor); CytD, cytochalasin D (actin inhibitor).

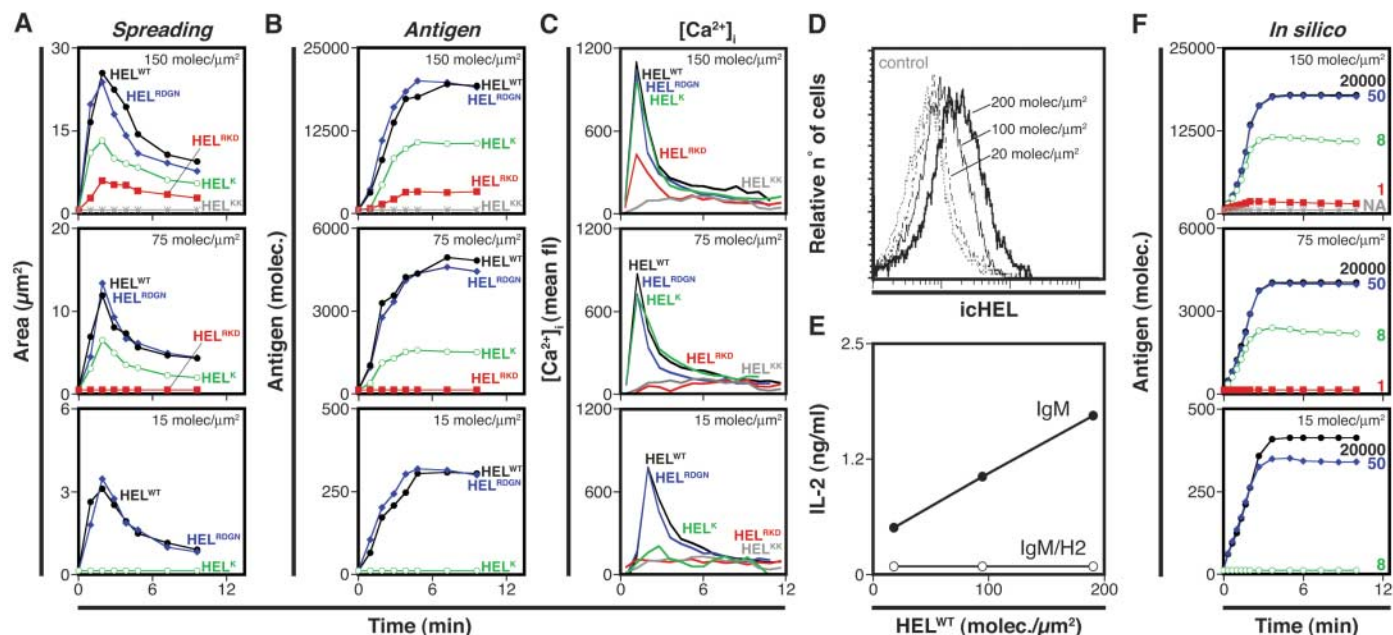


**Fig. 3.** The extent of B cell spreading depends on both the density and the affinity of the BCR for antigen and correlates with B cell activation. Kinetics of (A) B cell spreading, (B) antigen accumulation, and (C) the intracellular calcium response when MD4 transgenic B cells were settled on artificial planar bilayers loaded at the indicated densities with mutant HELs. Filled circles, HEL<sup>WT</sup> ( $K_a = 2.1 \times 10^{10} \text{ M}^{-1}$ ); Diamonds, HEL<sup>RDGN</sup> ( $K_a = 5.2 \times 10^7 \text{ M}^{-1}$ ); open circles, HEL<sup>K</sup> ( $K_a = 8.7 \times 10^6 \text{ M}^{-1}$ ); Squares, HEL<sup>RKD</sup> ( $K_a = 0.8 \times 10^6 \text{ M}^{-1}$ ); Asterisks, HEL<sup>KK</sup> ( $K_a < 0.4 \times 10^6 \text{ M}^{-1}$ ). (D) Uptake of Alexa488-conjugated HEL<sup>WT</sup> (icHEL) by MD4 B cells was

evaluated by flow cytometry after incubation on antigen-bearing membranes at the specified densities. (E) Antigen presentation of HEL-derived peptides by IgM (closed symbols) or IgM/H2 (open symbols) transfectants when settled together with HEL-specific 2G7 hybridoma T cells on lipid bilayers containing HEL<sup>WT</sup> at different densities. T cell activation was monitored by measuring interleukin-2 production after 24 hours. (F) Kinetics of antigen aggregation derived from the stochastic model. Antigen affinities are given as the affinity constant ( $K_a$ ) in  $\mu\text{M}^{-1}$  units. See also fig. S4.

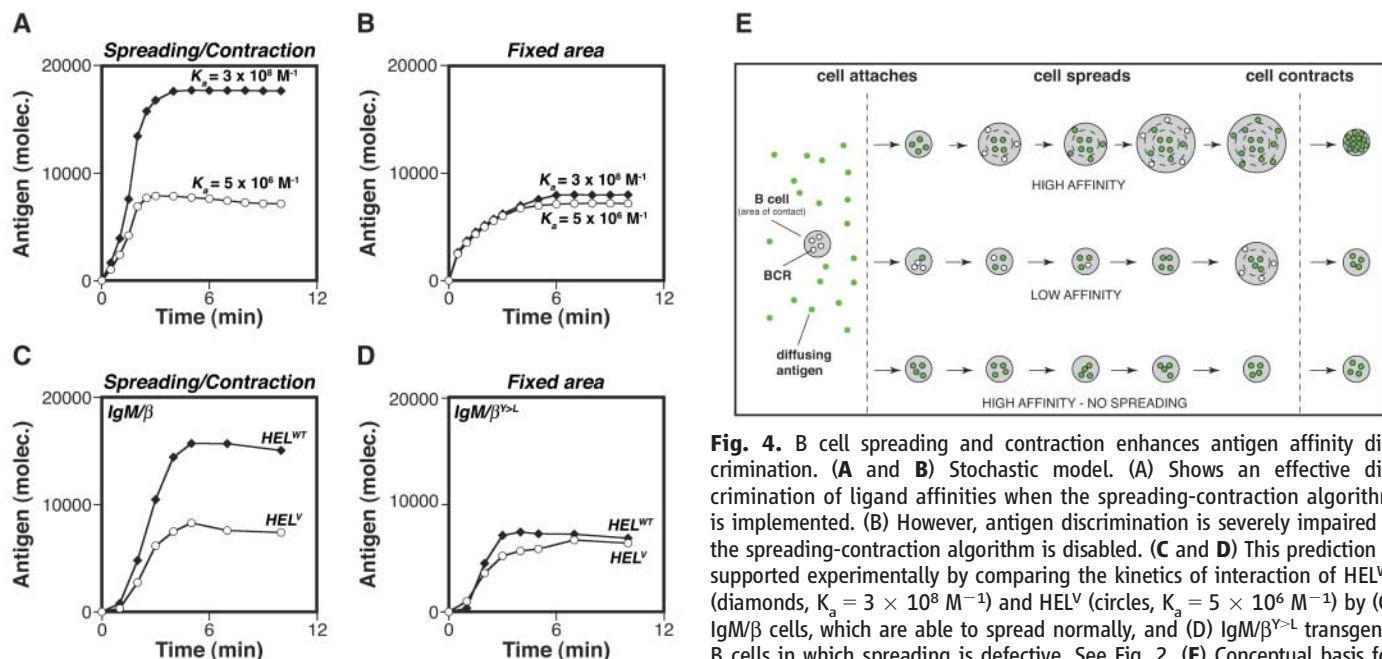


**Fig. 4.** B cell spreading and contraction enhances antigen affinity discrimination. (A and B) Stochastic model. (A) Shows an effective discrimination of ligand affinities when the spreading-contraction algorithm is implemented. (B) However, antigen discrimination is severely impaired if the spreading-contraction algorithm is disabled. (C and D) This prediction is supported experimentally by comparing the kinetics of interaction of HEL<sup>WT</sup> (diamonds,  $K_a = 3 \times 10^8 \text{ M}^{-1}$ ) and HEL<sup>L</sup> (circles,  $K_a = 5 \times 10^6 \text{ M}^{-1}$ ) by (C) IgM/β cells, which are able to spread normally, and (D) IgM/β<sup>Y-L</sup> transgenic B cells in which spreading is defective. See Fig. 2. (E) Conceptual basis for affinity discrimination. On the left, a B cell is shown that has just attached to a surface carrying diffusing antigens. If the interaction between antigen and BCR is of high affinity (upper row), rapid binding of antigen occurs. The high occupancy induces the cell to spread over the surface and expose more receptors, which in turn bind more antigen, leading to further spreading. After 2 min, the cell contracts and collects the receptor/ligand complexes into a central aggregate. However, if the interaction between antigen and receptors is of low affinity (middle row), binding occurs more slowly and the number of spreading events is much reduced. Consequently, when contraction takes place many fewer receptor-antigen complexes are collected. The lower row illustrates the situation in which the B cell is unable to spread because of a signaling-impaired BCR mutation. Even if high-affinity binding occurs, it cannot lead to an elevated accumulation of antigen.

a surface carrying diffusing antigens. If the interaction between antigen and BCR is of high affinity (upper row), rapid binding of antigen occurs. The high occupancy induces the cell to spread over the surface and expose more receptors, which in turn bind more antigen, leading to further spreading. After 2 min, the cell contracts and collects the receptor/ligand complexes into a central aggregate. However, if the interaction between antigen and receptors is of low affinity (middle row), binding occurs more slowly and the number of spreading events is much reduced. Consequently, when contraction takes place many fewer receptor-antigen complexes are collected. The lower row illustrates the situation in which the B cell is unable to spread because of a signaling-impaired BCR mutation. Even if high-affinity binding occurs, it cannot lead to an elevated accumulation of antigen.

ation of the two. All kinetic parameters were either directly determined, or derived from experimental measurements (supporting online text).

To model the spreading response, the area of contact between cell and bilayer increased in a series of small steps. The dependence on antigen binding was obtained by stipulating that each successive increment of cell area took place only if the receptor occupancy reached 75%. If this critical occupancy was not attained 1 min after initial attachment (an indication of insufficient antigen or avidity) then the cell “detached” and the simulation was aborted. As soon as receptor occupancy reached 75%, the area of cell attachment was increased by a fixed amount and a new cohort of receptors added. Iterated application of this strategy continued until 2 min after the initial contact with the lipid bilayer, when the area of cell contact began to shrink at a rate based on experimental measurements. Receptor-antigen pairs were collected into the central area (supporting online text).

We found that, given suitable parameters, this simple model was able to reproduce the essential features of the B cell response (Fig. 3F and fig. S4). It had a similar time course of spreading and contraction and it had a comparable capacity to discriminate between different antigen densities and affinities. The quantity of antigen accumulated showed a nonlinear relationship with affinity and density over a wide range (fig. S5A). However, if the spreading mechanism was inactivated in the program, for example by giving the B cell a fixed area of contact, then the amount of antigen accumulated was closely similar for both high- and low-affinity antigens (Fig. 4, A and B)—a result that we also found using the experimental set-up (Fig. 4, C and D, and fig. S2, G and H). These results are consistent with the notion that

a quantitative relationship between receptor occupancy and cell spreading may influence the observed cellular response (Fig. 4E). Mechanistic details of this linkage—the role played by the small focal clusters of receptors and how these are coupled to actin accumulation and tyrosine phosphorylation and hence the extension of lamellipodia—will require further collaboration between experiment and theory.

The B cell spreading reported here shares some similarities to the one observed in T cells (18–21). Both processes are sensitive to inhibitors of signaling and actin polymerization (20) and could represent an active process common to lymphocytes in general. In T cells, the process of antigen recognition has been the subject of extensive quantitative studies combined with computer models (22–25). However, the gathering of antigen by B cells is responsive to a much wider range of antigen affinities than T cells. It will occur in the absence of adhesion molecules without compromising the fundamental features of the antigen-specific responses. This highly reduced experimental system can then be modeled using a simple stochastic algorithm based on the binding interactions between antigen and cell receptors. In this way, we have been able to clarify the basis of the powerful discriminatory ability of B cells.

#### References and Notes

1. D. M. Russell *et al.*, *Nature* **354**, 308 (1991).
2. S. B. Hartley *et al.*, *Nature* **353**, 765 (1991).
3. J. G. Tew, M. H. Kosco, G. F. Burton, A. K. Szakal, *Immunol. Rev.* **117**, 185 (1990).
4. M. Wykes, A. Pombo, C. Jenkins, G. G. MacPherson, *J. Immunol.* **161**, 1313 (1998).
5. A. M. Haberman, M. J. Shlomchik, *Nat. Rev. Immunol.* **3**, 757 (2003).
6. M. H. Kosco-Vilbois, *Nat. Rev. Immunol.* **3**, 764 (2003).
7. A. Bergtold, D. D. Desai, A. Gavhane, R. Clynes, *Immunity* **23**, 503 (2005).

8. F. D. Batista, D. Iber, M. S. Neuberger, *Nature* **411**, 489 (2001).
9. Y. R. Carrasco, S. J. Fleire, T. Cameron, M. L. Dustin, F. D. Batista, *Immunity* **20**, 589 (2004).
10. C. R. Monks, B. A. Freiberg, H. Kupfer, N. Suciak, A. Kupfer, *Nature* **395**, 82 (1998).
11. A. Grakoui *et al.*, *Science* **285**, 221 (1999).
12. M. F. Krummel, M. D. Sjaastad, C. Wulfig, M. M. Davis, *Science* **289**, 1349 (2000).
13. C. C. Goodnow *et al.*, *Nature* **334**, 676 (1988).
14. Y. M. Teh, M. S. Neuberger, *J. Exp. Med.* **185**, 1753 (1997).
15. G. T. Williams, C. J. Peaker, K. J. Patel, M. S. Neuberger, *Proc. Natl. Acad. Sci. U.S.A.* **91**, 474 (1994).
16. M. Reth, *Nature* **338**, 383 (1989).
17. S. S. Andrews, D. Bray, *Phys. Biol.* **1**, 137 (2004).
18. S. C. Bunnell *et al.*, *J. Cell Biol.* **158**, 1263 (2002).
19. S. C. Bunnell, V. Kapoor, R. P. Triple, W. Zhang, L. E. Samelson, *Immunity* **14**, 315 (2001).
20. P. A. Negulescu, T. B. Krasieva, A. Khan, H. H. Kerschbaum, M. D. Cahalan, *Immunity* **4**, 421 (1996).
21. M. V. Parsey, G. K. Lewis, *J. Immunol.* **151**, 1881 (1993).
22. N. J. Burroughs, C. Wulfig, *Biophys. J.* **83**, 1784 (2002).
23. K. H. Lee *et al.*, *Science* **302**, 1218 (2003).
24. S. J. Lee, Y. Hori, J. T. Groves, M. L. Dustin, A. K. Chakraborty, *Trends Immunol.* **23**, 500 (2002).
25. Q. J. Li *et al.*, *Nat. Immunol.* **5**, 791 (2004).
26. We thank P. Bates and his group, J. Lewis, K. Lipkow, V. Silva-Vargas, and C. Reis e Sousa for critical reading of this manuscript. We also thank the Electron Microscopy Unit at the London Research Institute. This work was funded by National Institute of General Medical Sciences grant G64713 (D.B.), Cancer Research UK, and the European Molecular Biology Organization Young Investigator Program (F.D.B.).

#### Supporting Online Material

www.sciencemag.org/cgi/content/full/312/5774/738/DC1

Materials and Methods

SOM Text

Figs. S1 to S5

Table S1

References

Movies S1 to S4

16 December 2005; accepted 13 March 2006

10.1126/science.1123940

## Structure of the Multidrug Transporter EmrD from *Escherichia coli*

Yong Yin,\* Xiao He,\* Paul Szewczyk, That Nguyen, Geoffrey Chang†

EmrD is a multidrug transporter from the Major Facilitator Superfamily that expels amphipathic compounds across the inner membrane of *Escherichia coli*. Here, we report the x-ray structure of EmrD determined to a resolution of 3.5 angstroms. The structure reveals an interior that is composed mostly of hydrophobic residues, which is consistent with its role transporting amphipathic molecules. Two long loops extend into the inner leaflet side of the cell membrane. This region can serve to recognize and bind substrate directly from the lipid bilayer. We propose that multisubstrate specificity, binding, and transport are facilitated by these loop regions and the internal cavity.

The advent of medicinal antibiotics heralded an unprecedented breakthrough in the treatment of infectious disease, but the emergence of drug-resistant bacteria is threatening to undermine this achievement. Multidrug resistance (MDR) develops partially through direct drug efflux by integral mem-

brane transporters. There are two classes of MDR transporters: adenosine 5'-triphosphate (ATP)-binding cassette (ABC) proteins that directly couple drug efflux to ATP hydrolysis and secondary transporters that use energy derived from electrochemical gradients across the cell membrane. The secondary transporters in-

clude four families: the Resistance/Nodulation/Division superfamily (RND), the Multiple Antimicrobial Toxin Extrusion family, the Small Multidrug Resistance family, and the Major Facilitator Superfamily (MFS). The MDR transporters from the MFS family (MDR MFS) are among the most prevalent in microbial genomes and diverse in their substrate specificities (1).

One MDR MFS transporter, EmrD, is a proton-dependent secondary transporter from *Escherichia coli*. EmrD was first identified as an efflux pump for uncouplers of oxidative phosphorylation (2), which can rapidly arrest growth in bacteria by depleting the H<sup>+</sup> gradient (3). Some of these uncouplers are structurally unrelated, such as meta-chloro carbonylcyanide

The Scripps Research Institute, Department of Molecular Biology, 10550 North Torrey Pines Road, CB-105, La Jolla, CA 92037, USA.

\*These authors contributed equally to this work.

†To whom correspondence should be addressed. E-mail: gchang@scripps.edu